HHS Public Access

Author manuscript

Acta Neuropathol. Author manuscript; available in PMC 2016 March 03.

Published in final edited form as:

Acta Neuropathol. 2015 October ; 130(4): 587–597. doi:10.1007/s00401-015-1470-8.

Genetic, epigenetic, and molecular landscapes of multifocal and multicentric glioblastoma

Qun Liu[1,4], **Yuexin Liu**[1], **Wenliang Li**[4], **Xiaoguang Wang**[4], **Raymond Sawaya**[2], **Frederick F. Lang**[2], **W.K. Alfred Yung**[3], **Kexin Chen**[5], **Gregory N. Fuller**[1], and **Wei Zhang**[1]

[1]Department of Pathology, The University of Texas MD Anderson Cancer Center, Houston, Texas, USA

[2]Department of Neurosurgery, The University of Texas MD Anderson Cancer Center, Houston, Texas, USA

[3]Department of Neuro-Oncology, The University of Texas MD Anderson Cancer Center, Houston, Texas, USA

[4]Department of Neurosurgery, National Clinical Research Center for Cancer, Key Laboratory of Cancer Prevention and Therapy of Tianjin, Tianjin Medical University Cancer Hospital and Institute, Tianjin, PR China

[5]Department of Epidemiology and Biostatistics, National Clinical Research Center for Cancer, Key Laboratory of Cancer Prevention and Therapy of Tianjin, Tianjin Medical University Cancer Hospital and Institute, Tianjin, PR China

Abstract

Ten to twenty percent of newly diagnosed glioblastoma (GBM) patients initially present with multiple lesions, termed multifocal or multicentric GBM (M-GBM). The prognosis of these patients is poorer than is that of solitary GBM (S-GBM) patients. However, it is unknown whether multifocality has a genetic, epigenetic, or molecular basis. Here, we identified the genetic and epigenetic characteristics of M-GBM by performing a comprehensive analysis of multidimensional data, including imaging, genetic, epigenetic, and gene expression profiles, from 30 M-GBM cases in The Cancer Genome Atlas (TCGA) database and comparing the results with those of 173 S-GBM cases. We found that M-GBMs had no *IDH1*, *ATRX*, or *PDGFRA* mutations and were significantly associated with the mesenchymal subtype. We also identified the *CYB5R2* gene to be hypo-methylated and overexpressed in M-GBMs. The expression level of *CYB5R2* was significantly associated with patient survival in two major independent GBM cohorts, totaling 758 cases. The *IDH1* mutation was markedly associated with *CYB5R2* promoter methylation, but the survival influence of *CYB5R2* was independent of *IDH1* mutation status. *CYB5R2* expression was significantly associated with collagen maturation and the catabolic process and immunoregulation pathways. These results reveal that M-GBMs have some underlying genetic and epigenetic

Correspondence: Wei Zhang, PhD, Department of Pathology, Unit 85, The University of Texas MD Anderson Cancer Center, 1515 Holcombe Blvd., Houston, TX 77030; telephone: 713-745-1103; fax: 713-792-5549; wzhang@mdanderson.org..

The authors disclose no potential conflicts of interest.

characteristics that are associated with poor prognosis and that *CYB5R2* is a new epigenetic marker for GBM prognosis.

Keywords

Multifocal glioma; multicentric glioma; magnetic resonance imaging; isocitrate dehydrogenase 1; cytochrome b5 reductase 2; mutation; DNA methylation

Introduction

Glioblastoma (GBM) is the most common and most uniformly fatal cancer originating in the central nervous system [1]. Currently, surgical resection and radiotherapy, combined with adjuvant temozolomide (TMZ) chemotherapy, are standard treatment strategies for this disease [30]. However, despite our increased understanding of the oncological mechanisms that underlie the pathophysiological characteristics of GBM and despite the use of TMZ, the prognosis of the disease remains very poor, with a median patient survival duration of 15 to 17 months [17].

There are several reasons for the dismal prognosis of GBM patients. The disease's invasive nature makes complete resection difficult. In addition, it is often resistant to radiotherapy and chemotherapy, which invariably leads to local recurrence, the primary cause of treatment failure. GBM that is refractory to surgery, radiotherapy, and chemotherapy is especially challenging in the 10%-20% of patients who have multiple lesions on presentation [10, 11]; these patients usually experience a poorer outcome than do those with solitary lesions. Recent therapeutic advances have not slowed disease progression or improved survival durations in this group of GBM patients [14].

The genetic, epigenetic, and molecular characteristics may explain the poor outcomes found in patients with multifocal and multicentric GBM (M-GBM). However, the exact pathogenic mechanisms of multifocality are unknown [24], although it is presumed that malignant glial cells in M-GBM have an increased ability to disseminate compared with S-GBM. Given the diffuse and invasive nature of M-GBM, advances in focal therapies have had little impact on outcomes. Furthermore, the biologic characteristics of M-GBM, with its inherent ability to migrate and invade, may portend the poor survival duration observed in these patients. Identifying the molecular mechanism of M-GBM may not only provide critical information for developing new therapeutic strategies for this group of GBM patients but also give us an opportunity to understand the pathogenesis of GBM progression.

We identified the genetic and epigenetic characteristics of M-GBM by performing a comprehensive analysis of clinical, imaging, and genome data, provided by The Cancer Genome Atlas (TCGA), and comparing the results with those of S-GBM cases.

Methods

Patient population and MRI classification

We identified all treatment-naïve GBM patients for whom pretreatment MRIs were available in the National Cancer Institute's The Cancer Imaging Archive (http://cancerimagingarchive.net/). All patients had been diagnosed between 1997 and 2011. First, we divided the GBM cases into two subgroups by MRI findings: solitary glioblastoma (S-GBM), with one enhancing tumor, and M-GBM, with at least two clearly separated foci of enhancing tumors (Supplemental Figure 1); this group included two types, multifocal and multicentric GBM. The centers of multicentric GBM belong to different lobes or bilateral brains, with no apparent route of dissemination. The centers of multifocal GBM may only be a short distance apart, suggesting that the tumor cells migrate elsewhere and develop into a new tumor center (Fig. 1a). The study was approved by the institutional review board at The University of Texas MD Anderson Cancer Center.

Clinical and molecular data

The clinical and molecular data for this study were downloaded from the TCGA data portal (http://cancergenome.nih.gov/dataportal) on December 1, 2014. The clinical variables were age at diagnosis, sex, and Karnofsky performance score (KPS), and the treatment variables were radiotherapy and chemotherapy with temozolomide (TMZ) and "other drugs"; each treatment status was presented as a binary variable indicating whether the given treatment had been received. The molecular data used included somatic mutations, copy number alterations, DNA methylation, and mRNA expression. For somatic mutations, we used level 3 data, which indicated whether a mutation had occurred in a given gene. For the DNA copy number, the level 3 Affymetrix SNP6 data were mapped to the UCSC hg18 version of the human genome and a mean value was calculated for each chromosomal cytoband according to UCSC (http://hgdownload.cse.ucsc.edu/goldenpath/hg18/database/). The copy number alteration magnitudes of gene and cytoband levels were classified using simple thresholds: deletion ($\times < -1$), partial deletion ($-1 < \times < -0.7$), loss ($\times < -0.2$), gain ($0.2 < \times < 1$), intermediate amplification ($1 < \times < 2$), or amplification ($\times > 2$). For DNA methylation, the common probes of level 3 HumanMethylation27 and HumanMethylation450 array data were used; these beta values represent methylated probe intensity divided by methylated probe intensity plus unmethylated probe intensity. We transformed these values into M-values to make the methylation value distribution normal and to enable us to use the t-test to determine the significance of methylation changes [16]. For mRNA expression, we used level 3 data from the Affymetrix HGU-133A array, which had already been processed and summarized [16].

REMBRANDT data were downloaded from the caArray archive (https://array.nci.nih.gov/caarray/project/fine-00037) as raw CEL files. A Robust Multi-array Average (RMA) procedure was performed using a gene-based probe set for the HG-U133-Plus2 platform and the R Affy package [8].

Biostatistical survival analysis and classification analysis

A proportional hazards regression analysis was performed using each covariate as a predictor of survival. For the gene level survival analysis, we divided the corresponding cohorts by the median gene expression level (low or high) of the gene of interest. We then used a log-rank test to compare the survival durations between the two groups. The O-6-methylguanine-DNA methyltransferase (MGMT) status and the four-TCGA subgroup classification were provided by the TCGA [4]. For those samples without MGMT status, we used level 1 methylation data, downloaded from the TCGA, to calculate the MGMT-STP27 score [2]. The samples with scores lower than 0.358 were classified as MGMT negative; the others were classified as MGMT positive.

Pathway analysis

We downloaded Gene Ontology human gene set data from www.geneontology.org since it is the most comprehensive gene annotation database. We filtered out annotations with the evidence code “IEA”, which is not very reliable [9]. We also filtered out the gene sets smaller than 20 and larger than 600. We then put the gene sets into Gene Set Enrichment Analysis (GSEA) software, which was downloaded from the Broad Institute [26]. We used gene expression data to calculate the normalized enrichment score (NES) for each gene set. To filter out the duplicated gene set, we calculated the unweighted Cohen’s kappa statistics between each of the two gene sets using the genes located in the leading edge. The gene sets that had kappa statistics over 0.6 were filtered out.

The differentially expressed gene analysis was conducted using the R limma package [22]. To evaluate the relationship between *CYB5R2* and the top dysregulated pathways, we calculated the mean Pearson's correlation coefficient of *CYB5R2* and genes in the leading edge of top 20 gene sets, ranked by the FDR q value. The P values were calculated using the permutation test for each gene set. In particular, we randomly permuted the *CYB5R2* expression level and calculated the mean Pearson's correlation coefficient for each gene set.

Results

Clinical characteristics of the study cohort

Among 258 GBM patients with available MRI data in The Cancer Imaging Archive, there were 224 newly diagnosed GBM patients with preoperative MRIs. In these patients, the incidence of M-GBM (combined multifocal and multicentric cases) on presentation was 15.6% (35 of 224). Twelve (34%) of these 35 cases could be further classified as multicentric, with widely separated foci in different lobes with no apparent route of dissemination (Fig. 1a). In seven (58%) of these 12 patients, tumors were located in the same cerebral hemisphere but different lobes. Among the four patients with tumors in both cerebral hemispheres, one tumor was found to cross the corpus callosum.

There is no known clinical relevance to the distinction between multifocal and multicentric GBMs [18]. In our study, 34.3% (12 of 35) of the tumors were multicentric, but given the small number of patients and the questionable clinical utility of this distinction, we combined the two types of multiple tumors (M-GBMs) to compare them with S-GBMs.

Two hundred three cases (30 M-GBMs and 173 S-GBMs) had available clinical information and data for gene expression, copy number, or mutation and were thus included in a further analysis. The median age of patients with M-GBM was 58.5 years; 72.7% had KPS scores of $\geqslant$ 80, 90% underwent tumor resection, and 10% underwent excisional biopsy. Radiotherapy was administered in 24 (86%) of 28 patients, with M-GBM and TMZ prescribed in 13 (57%) of 23. The clinical characteristics of the M-GBM and S-GBM patients in this study are summarized in Table 1.

M-GBM is associated with the mesenchymal subtype

The survival of patients in the M-GBM group was significantly poorer than that of patients in the S-GBM group (p = 0.001, Cox regression analysis; Fig. 1b), consistent with the findings of previous reports [10, 25]. The TCGA working group described four subtypes of GBM (classic, mesenchymal, proneural, and neural) and defined the CpG island methylation unique subtype (G-CIMP) as a subtype of the proneural group [4]. Our analysis showed that the mesenchymal subtype dominated in the M-GBM group (p = 0.03; mesenchymal versus others) (Fig. 1c). Interestingly, there were no G-CIMP cases in the M-GBM group, although this result was not significant (p = 0.22) (likely due to the small sample size).

Genetic landscape of M-GBM

We analyzed the 103 cases for which mutation data were available (18 cases of M-GBM and 85 cases of S-GBM) (Fig. 2). Mutations in *IDH1*, *ATRX*, and *PDGFRA* were not present in the M-GBM group, which was consistent with their classification: these mutations are most commonly associated with the proneural group or the G-CIMP subgroup. In our analysis, among the M-GBMs for which mutation data were available, only three were proneural and none were G-CIMP. The number of TP53 mutations did not differ between M-GBM and S-GBM cases (p = 0.86).

The copy number change results are presented in Figure 3. A copy number analysis of the cytoband level showed that 6q13-q27, 9q34.11, 17q11.2, 17q21.32-q21.33, and 17q24.3 had differing copy number profiles between M-GBM and S-GBM. The copy number change at the gene level showed that most genes with P values lower than 0.05 were located in these chromosome locations. However, after adjusting for FDR, the differences did not reach statistical significance (Supplemental Table 2).

M-GBM is associated with *CYB5R2* as a novel prognostic gene

To understand the molecular mechanism of M-GBM development, we performed a pathway analysis using the GSEA method with the GO gene set. The immunoresponse, cytoskeletal, mitochondrial respiration, collagen decomposition, lipid kinase, and tumor necrosis factor pathways were all enriched in M-GBM (Fig. 4).

To gain further insight into the possible driver genes of M-GBM, we identified 45 genes that were significantly differentially expressed (FDR < 0.25) in the M-GBM group compared with in the S-GBM group (Supplemental Table 3, Supplemental Figure 2). Next, we compared the copy number change and methylation status of these genes between the two

subgroups (Supplemental Table 4). The most differentially expressed genes also showed the most differences in methylation levels (Fig. 5a, Supplemental Figure 3b).

Among those 45 genes, *CYB5R2* exhibited the most significant differences in gene expression, promoter methylation, and copy number alteration. The methylation level of cg03826976, which is located in the CpG island of the CYB5R2 promoter, was significantly lower in the M-GBM group (P = 0.007, Welch t test) (Fig. 5b). The methylation of cg03826976 was negatively correlated with the expression of *CYB5R2* (P = 0.0004, linear regression) (Fig. 5c). When we had used all available TCGA samples (not just those for which MRI data were available), the expression levels of *CYB5R2* were found to be associated with overall survival (P = 0.00018, log-rank test) (Fig. 5d). This survival association was validated in the REMBRANDT cohort, and higher expression of *CYB5R2* was similarly correlated with a shorter survival duration, independent of tumor grade (Fig. 6a,b, Supplemental Figure 4).

IDH1 mutations are associated with methylation of the CYB5R2 promoter

Higher *IDH1* mutation rates are associated with grade II and III astrocytomas and oligodendrogliomas and secondary GBM [21, 29]. *IDH1* mutations were also highly correlated with global promoter hypermethylation of CpG islands [28]. Therefore, we further explored the relationship between the methylation of CYB5R2 promoter CpG islands and IDH1 mutation. The results showed that *IDH1* mutations were correlated with CYB5R2 promoter methylation ($P = 1.2 \times 10^{-10}$, Fig. 6d, Supplemental Figure 3b) and expression level ($P = 5.4 \times 10^{-12}$, Fig. 6e). To determine whether the survival effect of *CYB5R2* could be attributed to *IDH1* mutations, we performed a survival analysis in *IDH1* wild-type samples. High expression of *CYB5R2* was still significantly correlated with poor survival (P = 0.015, log-rank test) (Fig. 6f).

CYB5R2 is associated with many critical pathways for M-GBM

The role of *CYB5R2*, a NADH-cytochrome b5 reductase, in cancer is poorly understood. Therefore, we analyzed the relationship between *CYB5R2* and activated cancer pathways. We calculated the coefficient of correlation between *CYB5R2* and genes located in the leading edge of active pathways. The pathways were ranked by the mean value of the coefficient of correlation. Figure 7 shows that the mean coefficient of correlation between *CYB5R2* and the genes in three pathways was over 0.2. *CYB5R2* is highly correlated with many proteases, including the MMP family, CTS family, and toll receptor family, that are known to be important for tumor invasion.

Discussion

GBM has one of the shortest survival durations of all cancers. MRI identifies a subgroup of patients with multiple lesions (termed M-GBMs in this study) that has even poorer survival. Although the genetic and epigenetic landscapes of GBM have been extensively interrogated, it is unknown whether M-GBMs have unique genetic and epigenetic characteristics that can be used as targets for future intervention.

In this study, we examined the MRI information in the TCGA database and identified 35 (15.6%) M-GBMs. In the literature, the reported incidence of multiple lesions at the time of diagnosis ranges from 0.5% to 35%, depending on the criteria [11, 15, 27]. More recent studies using a definition similar to ours documented M-GBM rates of 10%–15% [18]. After controlling for age, KPS score, MGMT status, and treatment, we showed that M-GBM cases in the TCGA cohort had significantly shorter survival durations than did S-GBM cases (6 months vs 11 months, respectively). Thus, M-GBMs represent the most deadly subgroup of GBMs.

Our analysis revealed some underlying features of M-GBMs. We showed that almost half (47%) the M-GBMs belonged to the mesenchymal subtype, as defined by the TCGA. No M-GBMs belonged to the G-CIMP subgroup. Paulsson et al [19] reported a similar classification trend in the eight M-GBMs among the 41 GBM patients in their study. In their cohort, five (63%) were of the mesenchymal subtype, and none were of the G-CIMP subtype.

The systematic mutational, methylation, and gene expression differences between M-GBM and S-GBM have not been adequately examined, and few studies have evaluated specific tumor markers in M-GBM. Patil et al. [13] analyzed phosphorylated MAPK, PTEN, MGMT, and laminin b1 and b2 expression and EGFR amplification in S-GBM and M-GBM; they found no significant differences. In the TCGA cohort, M-GBMs exhibited no *IDH1*, *ATRX*, or *PDGFRA* mutation. *IDH1* mutation has been reported to be correlated with sign of invasion on MRI. A report by Carrillo et al. [5] that focused exclusively on GBMs showed that large tumor size, the presence of cysts, and the presence of satellites were all correlated with *IDH1* mutant tumors. However, the authors did not provide details about the incidence of M-GBMs, and the number of *IDH1* mutation cases was quite small (14 of 202). Baldock [3] showed that *IDH1* mutation status was strongly correlated with the MRI-based invasion profile, as calculated from the relationship between T1Gd-enhancing volumes and T2 volumes and the pretreatment radial tumor velocity. Given the favorable survival role of *IDH1* mutation [13], the relationship between *IDH1* mutation and the invasive features of GBMs needs to be further investigated.

By determining the methylation status of promoter CpG islands of different genes, as well as copy number changes, we identified a lower methylation rate of *CYB5R2* promoter CpG islands and a higher expression level of *CYB5R2* in M-GBMs; these findings indicated that the methylation of *CYB5R2* serves as a biomarker for M-GBM.

It was previously reported that *CYB5R2* is hypermethylated in prostate and nasopharyngeal cancer compared to in normal tissue, suggesting that it plays a role as a tumor suppressor [7, 31]. Our data show that GBM has a lower expression level of *CYB5R2* than does normal brain tissue. However, this low expression level is clearly correlated with a longer survival duration. This discrepancy may be due to normal brain tissue containing a considerable proportion of neurons besides glial cells, whereas GBMs are enriched in tumorigenic glial cells.

Gene promoter methylation is critical for GBM [6]. The expression level of *CYB5R2* is highly associated with the methylation status of its promoter CpG islands. Our data show that *IDH1* mutation was significantly linked to the *CYB5R2* methylation level, yet the survival influence of *CYB5R2* was not dependent on the *IDH1* mutation, which means that the favorable survival of patients with *IDH1* mutation may be partly due to the hypermethylation of *CYB5R2*. Recent reports have shown that *IDH1* mutations are involved in collagen maturation and stability. In an animal model of *IDH1 R132H* mutation, mice were found to have higher levels of immature type IV collagen, which contributes to the integrity of the blood-brain barrier and is specifically found in the basement membrane between astrocytes and endothelial cells [23]. Our data show that *CYB5R2* is highly correlated with most collagen genes, as well as collagen-catabolic genes (Fig. 7).

The toll-like pathway plays a critical role in innate immune responses and participates in the first line of defense against invading pathogens, which is very important for tumor cell migration and survival in a new environment [20]. Our pathway analysis showed that many immunoresponse pathways are involved in M-GBM. We showed that *CYB5R2* expression was highly correlated with many genes of the toll-like pathway, indicating that *CYB5R2* also plays an important role in immunoregulation.

A significant association was found between c-Met expression and matrix metalloproteinases 2 and 9, which may explain the increase in invasive and multifocal features in these GBMs [12]. Our data show that MMP1 and MMP7 are included in the list of the top differentially expressed genes (fold changes of 1.72 and 1.84, respectively), and *CYB5R2* is highly correlated with the MMP family and other proteases, which is consistent with the important role of proteases, especially the MMP family, in GBM invasion.

Overall, this study provides the genomic landscape of M-GBM, which sheds light on the cause of its poor prognosis. The methylation status of *CYB5R2* promoter CpG islands may serve as a biomarker for M-GBM. The *CYB5R2* gene may play a key role in collagen maturation, the catabolic process, and immunoregulation. Modulation of CYB5R2 may represent a novel strategy to improve the survival of GBM patients. Further studies should validate the survival impact of *CYB5R2*, both *in vivo* and *in vitro*.

Supplementary Material

Refer to Web version on PubMed Central for supplementary material.

Acknowledgments

We thank Ms. Ann M. Sutton of the Department of Scientific Publications at The University of Texas MD Anderson Cancer Center for editing this manuscript. This work was partially supported by NIH grants CA141432, CA09850305, and U24CA143835 to WZ and an MD Anderson core grant from the National Cancer Institute (CA16672) and grants from the Program for Changjiang Scholars and Innovative Research Team in University in China (IRT_14R40) to KC. QL was supported by a grant from Tianjin Medical University Cancer Institute and Hospital.

References

1. Aldape K, Zadeh G, Mansouri S, Reifenberger G, Deimling von A. Glioblastoma: pathology, molecular mechanisms and markers. Acta Neuropathol. 2015; 129:829–848.10.1007/s00401-015-1432-1 [PubMed: 25943888]
2. Bady P, Sciuscio D, Diserens A-C, Bloch J, van den Bent MJ, Marosi C, Dietrich P-Y, Weller M, Mariani L, Heppner FL, Mcdonald DR, Lacombe D, Stupp R, Delorenzi M, Hegi ME. MGMT methylation analysis of glioblastoma on the Infinium methylation BeadChip identifies two distinct CpG regions associated with gene silencing and outcome, yielding a prediction model for comparisons across datasets, tumor grades, and CIMP-status. Acta Neuropathol. 2012; 124:547–560.10.1007/s00401-012-1016-2 [PubMed: 22810491]
3. Baldock AL, Yagle K, Born DE, Ahn S, Trister AD, Neal M, Johnston SK, Bridge CA, Basanta D, Scott J, Malone H, Sonabend AM, Canoll P, Mrugala MM, Rockhill JK, Rockne RC, Swanson KR. Invasion and proliferation kinetics in enhancing gliomas predict IDH1 mutation status. Neuro-oncology. 2014; 16:779–786.10.1093/neuonc/nou027 [PubMed: 24832620]
4. Brennan CW, Verhaak RGW, McKenna A, Campos B, Noushmehr H, Salama SR, Zheng S, Chakravarty D, Sanborn JZ, Berman SH, Beroukhim R, Bernard B, Wu C-J, Genovese G, Shmulevich I, Barnholtz-Sloan J, Zou L, Vegesna R, Shukla SA, Ciriello G, Yung WK, Zhang W, Sougnez C, Mikkelsen T, Aldape K, Bigner DD, Van Meir EG, Prados M, Sloan A, Black KL, Eschbacher J, Finocchiaro G, Friedman W, Andrews DW, Guha A, Iacocca M, O'Neill BP, Foltz G, Myers J, Weisenberger DJ, Penny R, Kucherlapati R, Perou CM, Hayes DN, Gibbs R, Marra M, Mills GB, Lander E, Spellman P, Wilson R, Sander C, Weinstein J, Meyerson M, Gabriel S, Laird PW, Haussler D, Getz G, Chin L, TCGA Research Network. The somatic genomic landscape of glioblastoma. Cell. 2013; 155:462–477.10.1016/j.cell.2013.09.034 [PubMed: 24120142]
5. Carrillo JA, Lai A, Nghiemphu PL, Kim HJ, Phillips HS, Kharbanda S, Moftakhar P, Lalaezari S, Yong W, Ellingson BM, Cloughesy TF, Pope WB. Relationship between tumor enhancement, edema, IDH1 mutational status, MGMT promoter methylation, and survival in glioblastoma. AJNR Am J Neuroradiol. 2012; 33:1349–1355.10.3174/ajnr.A2950 [PubMed: 22322613]
6. Cogdell D, Chung W, Liu Y, McDonald JM, Aldape K, Issa J-PJ, Fuller GN, Zhang W. Tumor-associated methylation of the putative tumor suppressor AJAP1 gene and association between decreased AJAP1 expression and shorter survival in patients with glioma. Chin J Cancer. 2011; 30:247–253. [PubMed: 21439246]
7. Devaney JM, Wang S, Funda S, Long J, Taghipour DJ, Tbaishat R, Furbert-Harris P, Ittmann M, Kwabi-Addo B. Identification of novel DNA-methylated genes that correlate with human prostate cancer and high-grade prostatic intraepithelial neoplasia. Prostate Cancer and Prostatic Diseases. 2013; 16:292–300.10.1038/pcan.2013.21 [PubMed: 23896626]
8. Gautier L, Cope L, Bolstad BM, Irizarry RA. affy--analysis of Affymetrix GeneChip data at the probe level. Bioinformatics. 2004; 20:307–315.10.1093/bioinformatics/btg405 [PubMed: 14960456]
9. Gene Ontology Consortium. Gene Ontology Consortium: going forward. Nucleic Acids Research. 2015; 43:D1049–56.10.1093/nar/gku1179 [PubMed: 25428369]
10. Giannopoulos S, Kyritsis AP. Diagnosis and management of multifocal gliomas. Oncology. 2010; 79:306–312.10.1159/000323492 [PubMed: 21412017]
11. Hassaneen W, Levine NB, Suki D, Salaskar AL, de Moura Lima A, McCutcheon IE, Prabhu SS, Lang FF, DeMonte F, Rao G, Weinberg JS, Wildrick DM, Aldape KD, Sawaya R. Multiple craniotomies in the management of multifocal and multicentric glioblastoma. Clinical article. J Neurosurg. 2011; 114:576–584.10.3171/2010.6.JNS091326 [PubMed: 20690813]
12. Kong D-S, Song S-Y, Kim D-H, Joo KM, Yoo J-S, Koh JS, Dong SM, Suh Y-L, Lee J-I, Park K, Kim JH, Nam D-H. Prognostic significance of c-Met expression in glioblastomas. Cancer. 2009; 115:140–148.10.1002/cncr.23972 [PubMed: 18973197]
13. Liu X-Y, Gerges N, Korshunov A, Sabha N, Khuong-Quang D-A, Fontebasso AM, Fleming A, Hadjadj D, Schwartzentruber J, Majewski J, Dong Z, Siegel P, Albrecht S, Croul S, Jones DT, Kool M, Tönjes M, Reifenberger G, Faury D, Zadeh G, Pfister S, Jabado N. Frequent ATRX mutations and loss of expression in adult diffuse astrocytic tumors carrying IDH1/IDH2 and TP53

mutations. Acta Neuropathol. 2012; 124:615–625.10.1007/s00401-012-1031-3 [PubMed: 22886134]

14. Lou E, Peters KB, Sumrall AL, Desjardins A, Reardon DA, Lipp ES, Herndon JE, Coan A, Bailey L, Turner S, Friedman HS, Vredenburgh JJ. Phase II trial of upfront bevacizumab and temozolomide for unresectable or multifocal glioblastoma. Cancer Medicine. 2013; 2:185–195.10.1002/cam4.58 [PubMed: 23634286]
15. McKenzie JT, Guarnaschelli JN, Vagal AS, Warnick RE, Breneman JC. Hypofractionated stereotactic radiotherapy for unifocal and multifocal recurrence of malignant gliomas. J Neurooncol. 2013; 113:403–409.10.1007/s11060-013-1126-2 [PubMed: 23589034]
16. McLendon R, Friedman A, Bigner D, Van Meir EG, Brat DJ, Mastrogianakis GM, et al. Comprehensive genomic characterization defines human glioblastoma genes and core pathways. Nature. 2008; 455:1061–1068.10.1038/nature07385 [PubMed: 18772890]
17. Omuro A, DeAngelis LM. Glioblastoma and other malignant gliomas: a clinical review. JAMA. 2013; 310:1842–1850.10.1001/jama.2013.280319 [PubMed: 24193082]
18. Patil CG, Yi A, Elramsisy A, Hu J, Mukherjee D, Irvin DK, Yu JS, Bannykh SI, Black KL, Nuño M. Prognosis of patients with multifocal glioblastoma: a case-control study. J Neurosurg. 2012; 117:705–711.10.3171/2012.7.JNS12147 [PubMed: 22920963]
19. Paulsson AK, Holmes JA, Peiffer AM, Miller LD, Liu W, Xu J, Hinson WH, Lesser GJ, Laxton AW, Tatter SB, Debinski W, Chan MD. Comparison of clinical outcomes and genomic characteristics of single focus and multifocal glioblastoma. J Neurooncol. 2014; 119:429–435.10.1007/s11060-014-1515-1 [PubMed: 24990827]
20. Pradere J-P, Dapito DH, Schwabe RF. The Yin and Yang of Toll-like receptors in cancer. Oncogene. 2014; 33:3485–3495.10.1038/onc.2013.302 [PubMed: 23934186]
21. Reuss DE, Sahm F, Schrimpf D, Wiestler B, Capper D, Koelsche C, Schweizer L, Korshunov A, Jones DTW, Hovestadt V, Mittelbronn M, Schittenhelm J, Herold-Mende C, Unterberg A, Platten M, Weller M, Wick W, Pfister SM, Deimling von A. ATRX and IDH1-R132H immunohistochemistry with subsequent copy number analysis and IDH sequencing as a basis for an “integrated” diagnostic approach for adult astrocytoma, oligodendroglioma and glioblastoma. Acta Neuropathol. 2015; 129:133–146.10.1007/s00401-014-1370-3 [PubMed: 25427834]
22. Ritchie ME, Phipson B, Wu D, Hu Y, Law CW, Shi W, Smyth GK. limma powers differential expression analyses for RNA-sequencing and microarray studies. Nucleic Acids Research. 2015; 43:e47.10.1093/nar/gkv007 [PubMed: 25605792]
23. Sasaki M, Knobbe CB, Itsumi M, Elia AJ, Harris IS, Chio IIC, Cairns RA, McCracken S, Wakeham A, Haight J, Ten AY, Snow B, Ueda T, Inoue S, Yamamoto K, Ko M, Rao A, Yen KE, Su SM, Mak TW. D-2-hydroxyglutarate produced by mutant IDH1 perturbs collagen maturation and basement membrane function. Genes Dev. 2012; 26:2038–2049.10.1101/gad.198200.112 [PubMed: 22925884]
24. Shakur SF, Bit-Ivan E, Watkin WG, Merrell RT, Farhat HI. Multifocal and Multicentric Glioblastoma with Leptomeningeal Gliomatosis: A Case Report and Review of the Literature. Case Reports in Medicine. 2013; 2013:1–8.10.1155/2013/132679
25. Showalter TN, Andrel J, Andrews DW, Curran WJ Jr. Daskalakis C, Werner-Wasik M. Multifocal Glioblastoma Multiforme: Prognostic Factors and Patterns of Progression. International Journal of Radiation Oncology*Biology*Physics. 2007; 69:820–824.10.1016/j.ijrobp.2007.03.045
26. Subramanian A, Tamayo P, Mootha VK, Mukherjee S, Ebert BL, Gillette MA, Paulovich A, Pomeroy SL, Golub TR, Lander ES, Mesirov JP. Gene set enrichment analysis: a knowledge-based approach for interpreting genome-wide expression profiles. Proc Natl Acad Sci USA. 2005; 102:15545–15550.10.1073/pnas.0506580102 [PubMed: 16199517]
27. Thomas RP, Xu LW, Lober RM, Li G, Nagpal S. The incidence and significance of multiple lesions in glioblastoma. J Neurooncol. 2013; 112:91–97.10.1007/s11060-012-1030-1 [PubMed: 23354652]
28. Turkalp Z, Karamchandani J, Das S. IDH mutation in glioma: new insights and promises for the future. JAMA Neurol. 2014; 71:1319–1325.10.1001/jamaneurol.2014.1205 [PubMed: 25155243]
29. Wesseling P, van den Bent M, Perry A. Oligodendroglioma: pathology, molecular mechanisms and markers. Acta Neuropathol. 2015; 129:809–827.10.1007/s00401-015-1424-1 [PubMed: 25943885]

30. Wolbers JG. Novel strategies in glioblastoma surgery aim at safe, supra-maximum resection in conjunction with local therapies. Chin J Cancer. 2014; 33:8–15.10.5732/cjc.013.10219 [PubMed: 24384236]

31. Xiao X, Zhao W, Tian F, Zhou X, Zhang J, Huang T, Hou B, Du C, Wang S, Mo Y, Yu N, Zhou S, You J, Zhang Z, Huang G, Zeng X. Cytochrome b5 reductase 2 is a novel candidate tumor suppressor gene frequently inactivated by promoter hypermethylation in human nasopharyngeal carcinoma. Tumour Biol. 2014; 35:3755–3763.10.1007/s13277-013-1497-1 [PubMed: 24338690]

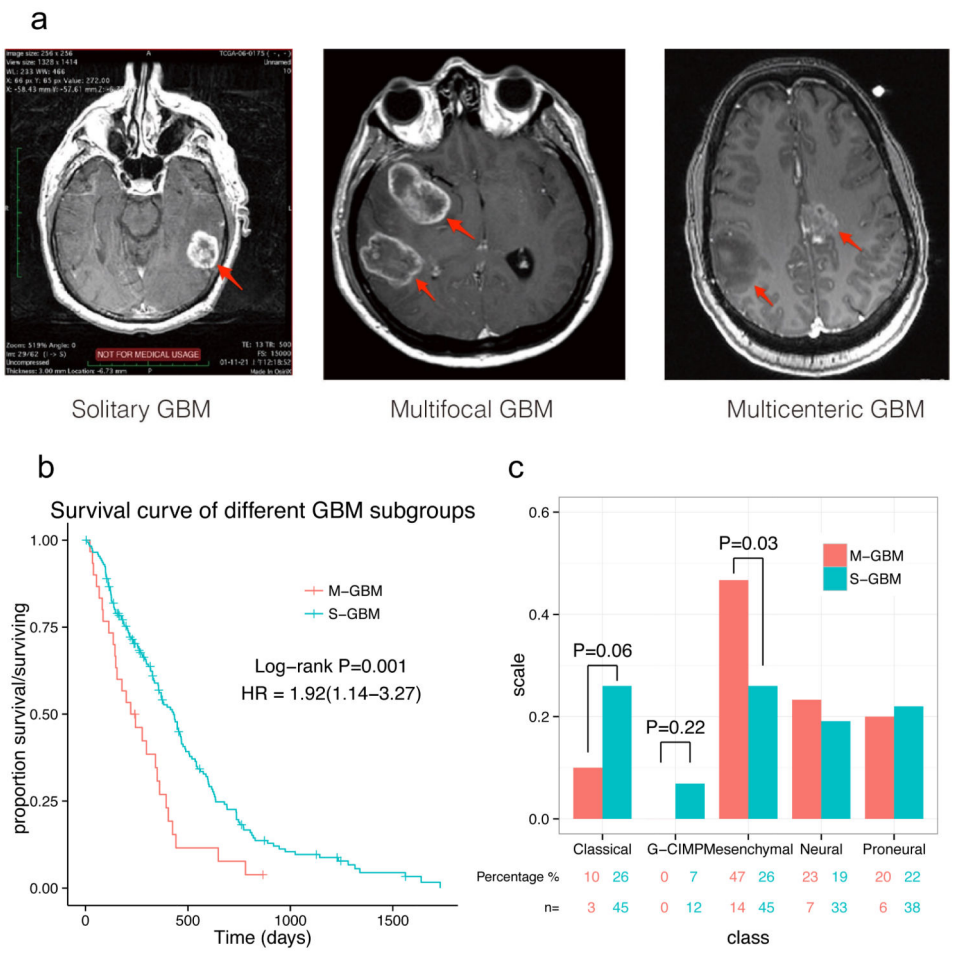

Figure 1. Survival and TCGA classification of two groups of GBM patients

(a) Typical MRIs of three GBM subgroups: S-GBM, multifocal GBM, and multicentric GBM. Multifocal and multicentric GBM were combined (M-GBM). (b) Kaplan–Meier survival curves comparing the survival durations of patients with S-GBM (median, 11 months) and M-GBM (median, 8 months). (c) The classification percentages of M-GBM and S-GBM. The mesenchymal subtype dominated in the M-GBM group (46.7%); the G-CIMP subtype was not found.

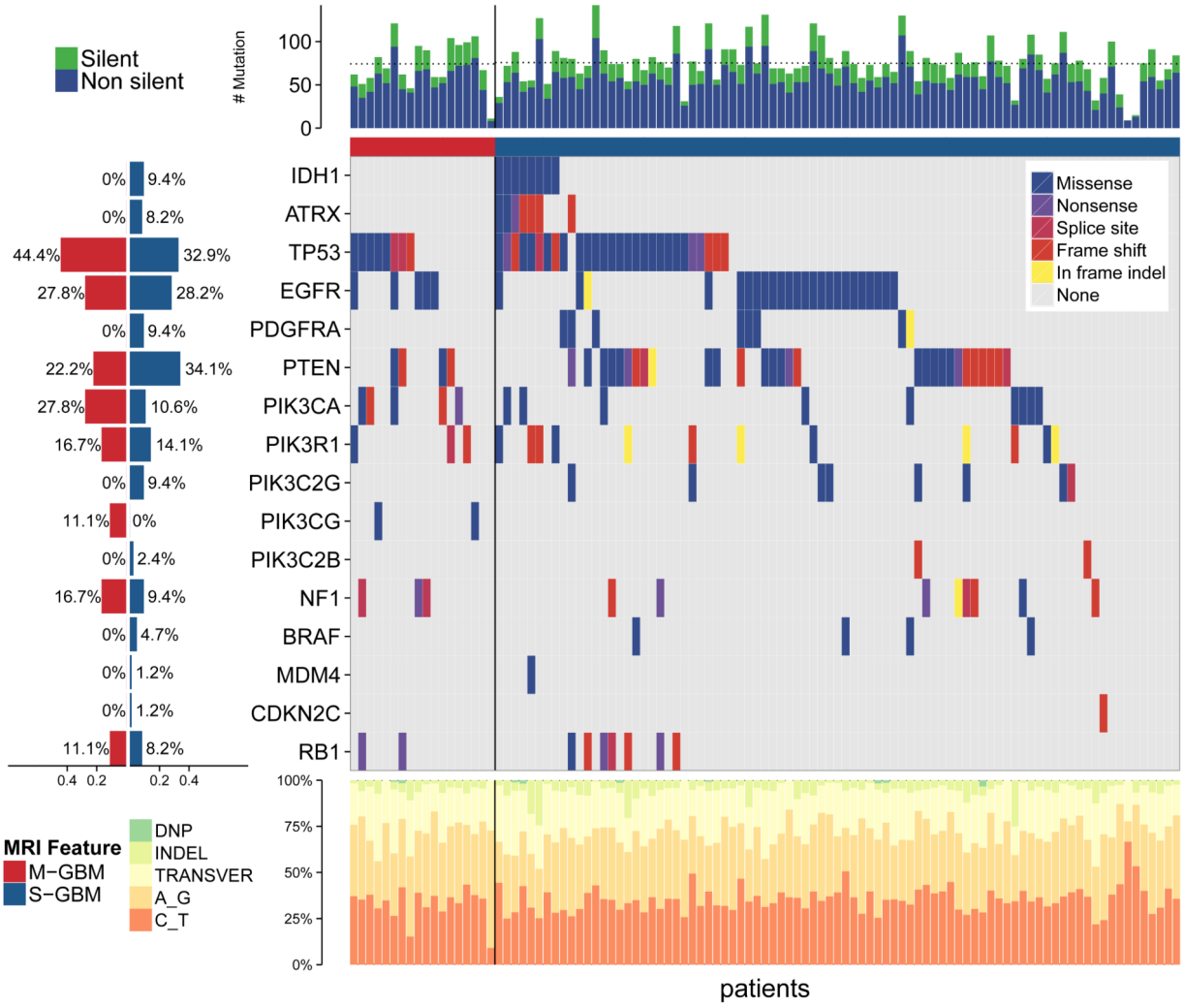

Figure 2. Gene mutation profiles of M-GBM and S-GBM

The upper panel shows that the total mutation numbers were not different between the two groups. The left panel shows the mutation proportion of the two groups, per the genes. The lower panel shows that the mutation spectra were not different between the two groups. The M-GBMs lacked *IDH1*, *ATRX*, and *PDGFRA*.

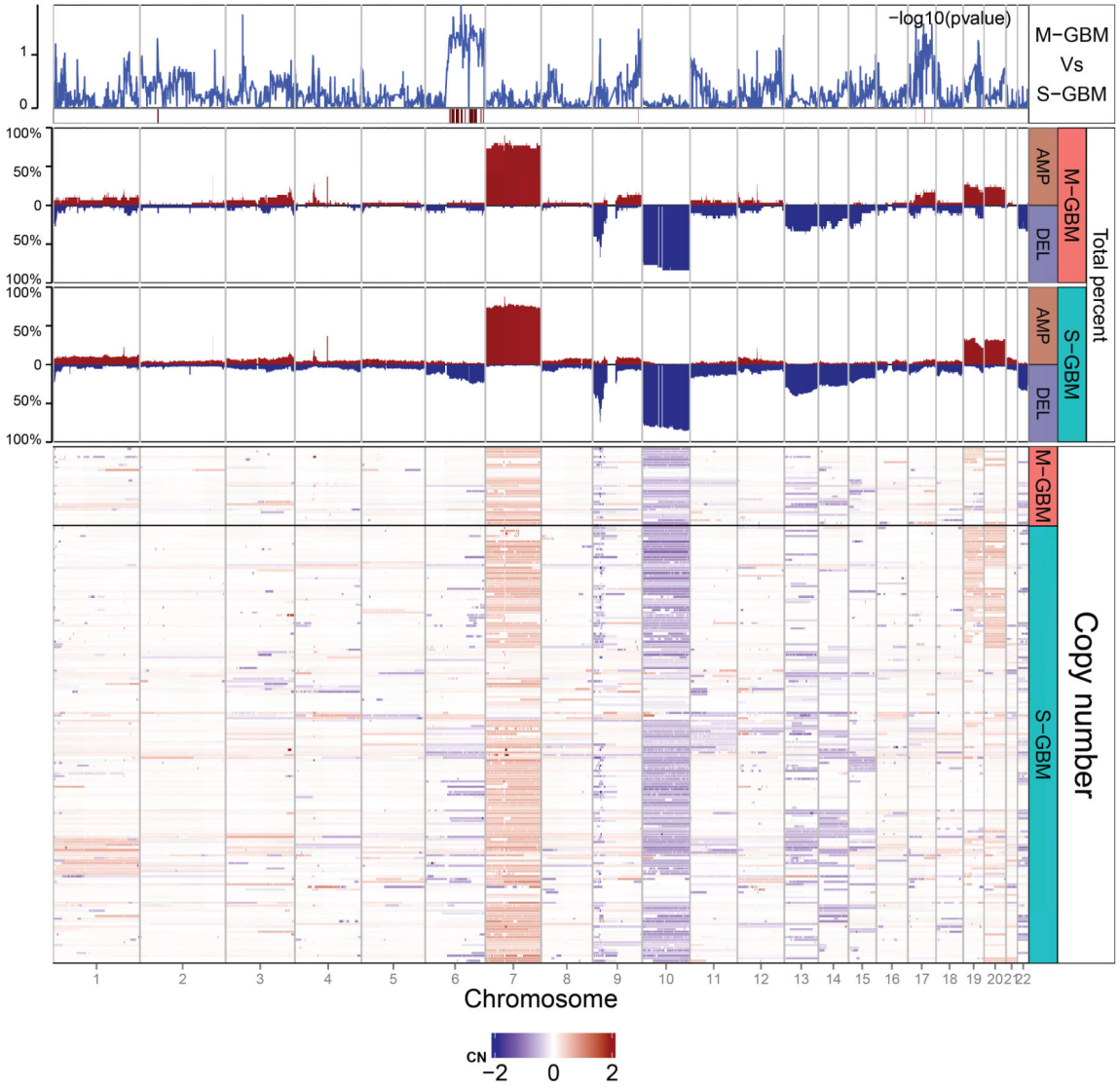

Figure 3. EGene copy number comparison of M-GBM and S-GBM

The bottom panel shows the copy number change profile of all samples. The center panel shows the copy number change proportion of the two subgroups. The top panel shows the P value of the logit regression of each chromosome region, and the red bars indicate the region with a P value below 0.05. After multiple test adjustments, the difference was not statistically significant.

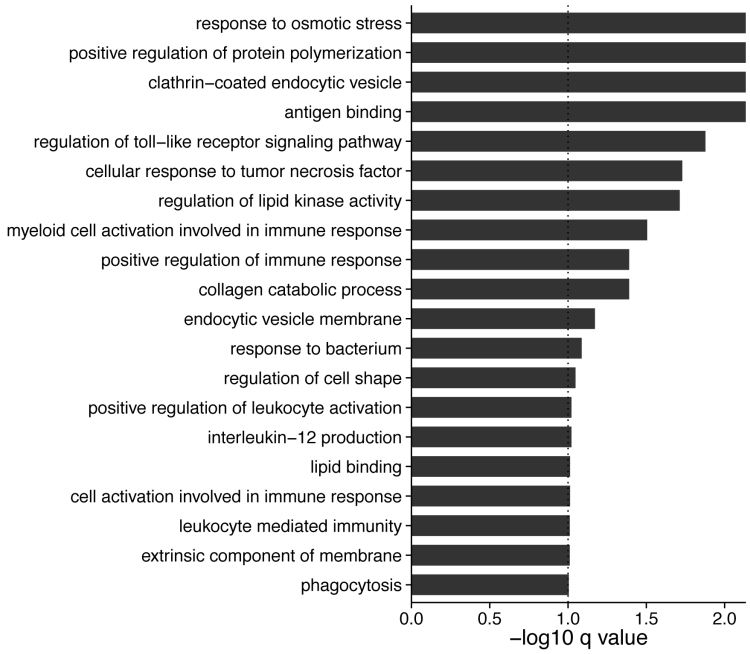

Figure 4. GSEA pathway analysis of M-GBM and S-GBM, ranked by NES

The duplicated gene sets are filtered out (kappa statistics > 0.60). The dotted line indicates an FDR q value equal to 0.1.

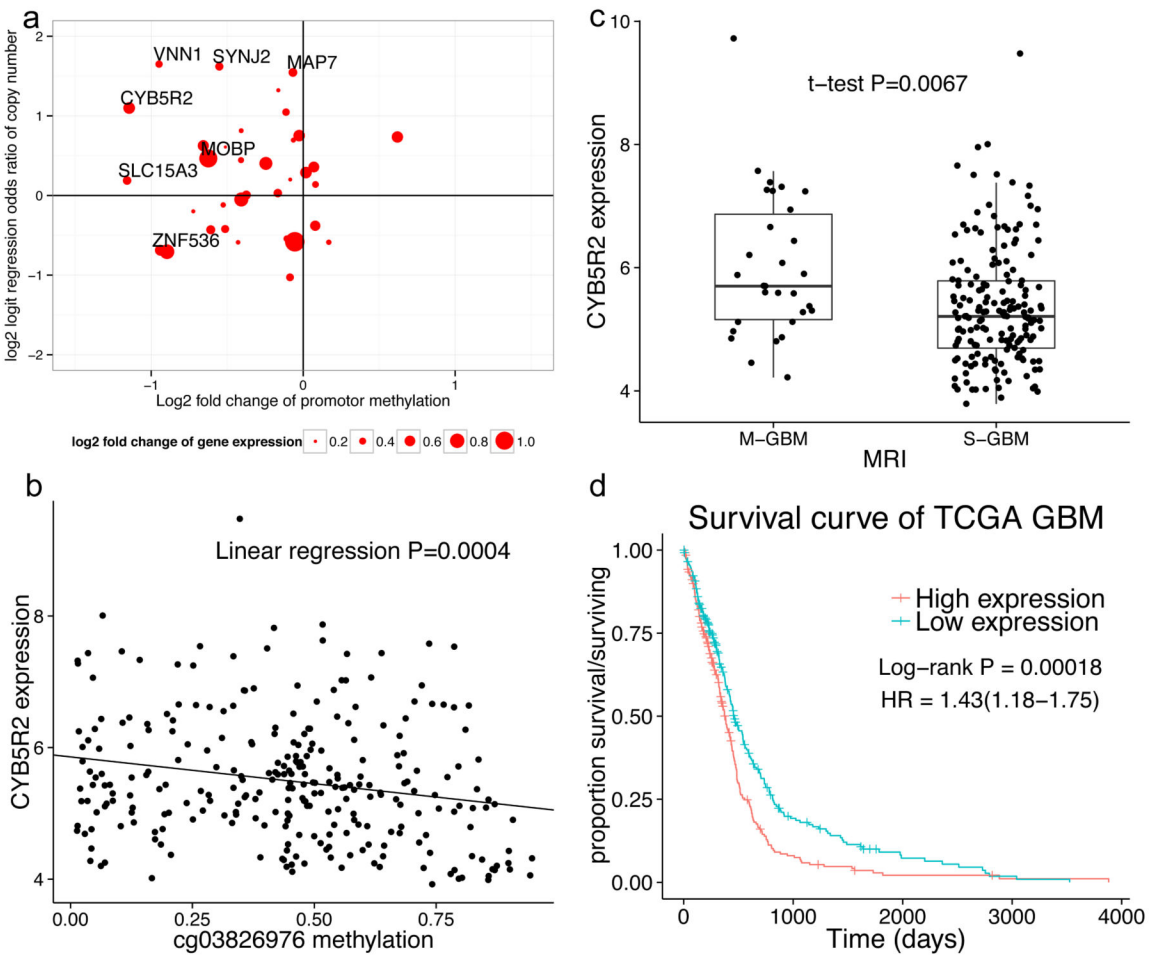

Figure 5. Methylation profile of M-GBM

(a) X axis indicates the log2-fold change of the promoter methylation between the two subgroups. The Y axis indicates the log2 logit regression odds ratio of the two groups for each gene. The size indicates the fold change of the gene expression level. The dots with names represent the genes with a p value of the copy number change or methylation level change lower than 0.05. (b) The methylation level of cg03826976 was negatively correlated with *CYB5R2* expression levels. (c) The M-GBM group had a higher mean expression level of *CYB5R2*. (d) The expression level of *CYB5R2* was negatively correlated with patient survival when patients were separated into two groups according to high and low expression, independent of S-GBM or M-GBM grouping.

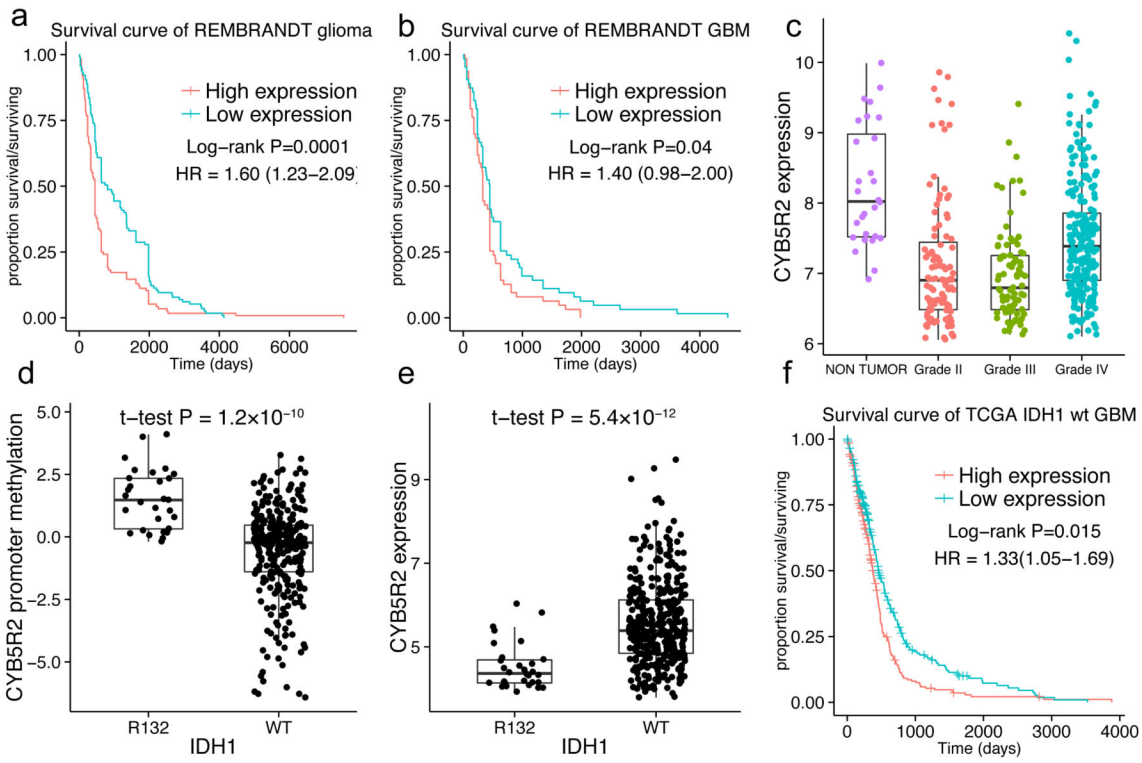

Figure 6. Validation of the correlation between *CYB5R2* and survival

(a) In the REMBRANDT database, the patients were divided into two groups by the median expression level of *CYB5R2*. The survival durations significantly differed. (b) In the REMBRANDT GBM cohort, a high expression level of *CYB5R2* was correlated with poor survival (P=0.03). (c) The expression level of *CYB5R2* in different GBM subgroups. A = astrocytoma (WHO grade II); AA = anaplastic astrocytoma (WHO grade III); O = oligodendroglioma (grade II); and AO = anaplastic oligodendroglioma (grade III). (d) The *IDH1* mutation was correlated with *CYB5R2* promoter methylation and reduced *CYB5R2* expression (e). (f) In the GBM group with wild-type IDH1, high expression of *CYB5R2* was indicative of poor survival.

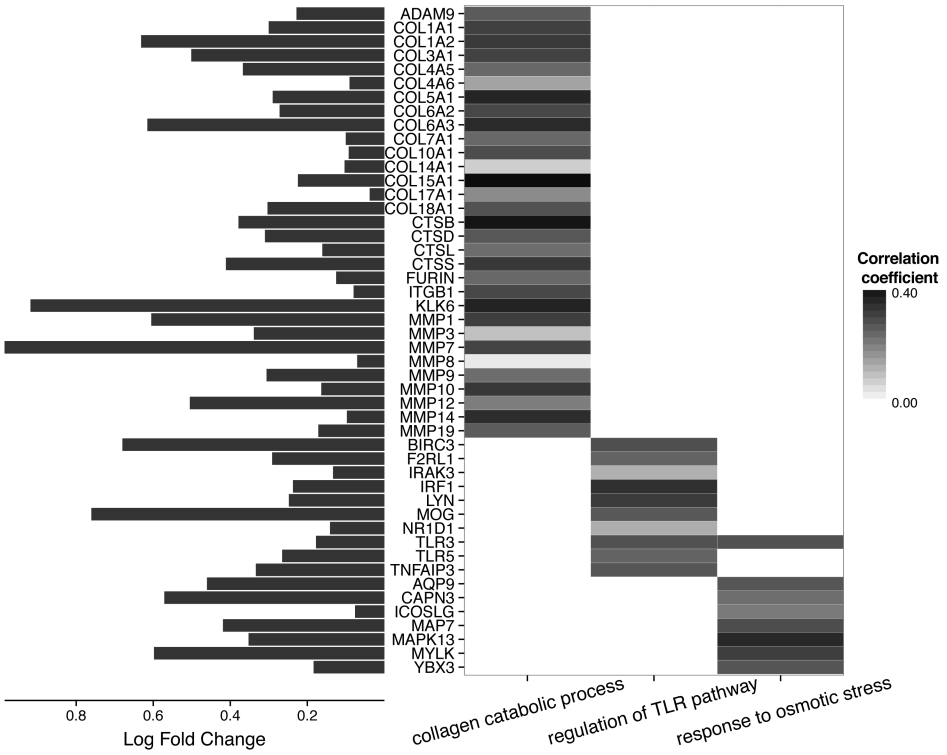

Figure 7. Pathway association of the *CYB5R2* gene

CYB5R2 expression was found to be correlated with three pathways based on the mean coefficient of correlation (over 0.2). The left panel shows the log2-fold change of those genes in M-GBM comparing to S-GBM. GO:0030574: collagen catabolic process ($P < 0.001$, permutation test); GO:0034121: toll–like receptor signaling pathway ($P < 0.001$, permutation test); and GO:0006970: response to osmotic stress ($P < 0.001$, permutation test).

Table 1

Demographic and clinical characteristics of study patients, including number of patients, age at diagnosis, sex, MGMT status, initial KPS score, and therapy

Characteristic	All GBM	S-GBM	M-GBM	P value
Number of patients, n (%)	203 (100)	173 (85.2)	30 (14.8)	-
Age at diagnosis, years (median)	61	61	58.5	0.88
Sex (male), n (%)	125 (61.6)	104 (60.1)	21 (70)	0.41
KPS score (mean)	77.7	78	76.4	0.67
MGMT promoter (methylated/available)	69/126	55/105	14/21	0.34
Resection (resection/available)	183/202	156/172	27/30	0.78
Radiotherapy (radiotherapy/available)	164/195	142/166	22/29	0.27
TMZ chemotherapy (TMZ/available)	105/151	92/128	13/23	0.15

MGMT, O-6-methylguanine-DNA methyltransferase; KPS, Karnofsky performance score; GBM, glioblastoma; S-GBM: solitary GBM; M-GBM, multifocal and multicentric GBM; TMZ, temozolomide.